Geophysical Research Letters

RESEARCH LETTER
10.1029/2024GL111669

# Disentangling Ecological Restoration's Impact on Terrestrial Water Storage

Xiaofan Shen[1,2], Liantao Niu[1,2], Xiaoxu Jia[1,2], Ting Yang[3], Wei Hu[4], Chaoyang Wu[2,5], Jiangdong Chu[6], Asim Biswas[7], and Ming'an Shao[1,2]

[1]Modern Agricultural Engineering Laboratory, Institute of Geographic Sciences and Natural Resources Research, Chinese Academy of Sciences, Beijing, China, [2]College of Resources and Environment, University of Chinese Academy of Sciences, Beijing, China, [3]Guangdong Provincial Key Laboratory of Remote Sensing and Geographical Information System, Guangzhou Institute of Geography, Guangdong Academy of Sciences, Guangzhou, China, [4]The New Zealand Institute for Plant and Food Research Limited, Christchurch, New Zealand, [5]Key Laboratory of Land Surface Pattern and Simulation, Institute of Geographical Sciences and Natural Resources Research, Chinese Academy of Sciences, Beijing, China, [6]College of Water Resources and Architectural Engineering, Northwest A&F University, Yangling, China, [7]School of Environmental Sciences, University of Guelph, Guelph, ON, Canada

Xiaofan Shen and Liantao Niu contributed equally to this work.

**Key Points:**

- New framework reveals overestimated impact of ER on water storage when mining and agriculture are ignored
- GRACE satellite data in Mu Us Sandyland is affected by coal mining, necessitating careful interpretation
- Comprehensive analysis shows farming consumes more water than ER, informing sustainable practices

**Supporting Information:**

Supporting Information may be found in the online version of this article.

**Correspondence to:**

X. Jia,
jiaxx@igsnrr.ac.cn

**Citation:**

Shen, X., Niu, L., Jia, X., Yang, T., Hu, W., Wu, C., et al. (2025). Disentangling ecological restoration's impact on terrestrial water storage. *Geophysical Research Letters*, *52*, e2024GL111669. https://doi.org/10.1029/2024GL111669

Received 1 AUG 2024
Accepted 29 JAN 2025



**Abstract** Large-scale ecological restoration (ER) in semiarid regions is often associated with substantial terrestrial water storage (TWS) depletion. This study challenged previous estimates by demonstrating the critical importance of considering other human activities when assessing ER impacts on TWS. Using a novel analytical framework integrating GRACE satellite data and ground observations, we analyzed TWS changes in China's Mu Us Sandyland under two scenarios: with and without considering mining and farming activities. Our results show that ER consumed TWS at an average rate of 11.7 ± 12.2 mm $yr^{-1}$ from 2003 to 2022. Neglecting the impacts of mining and farming led to a 251% overestimation of ER's effect on TWS. This study provided a more nuanced understanding of water resource dynamics in restored ecosystems, emphasizing the need for comprehensive approaches in TWS assessments and informing sustainable land management strategies globally.

**Plain Language Summary** Planting trees and restoring landscapes, known as ecological restoration (ER), helps mitigate climate change and improve dry environments. However, some are concerned that these efforts may delete significant amounts of water, exacerbating the strain on already limited water resources. Our study took a fresh look at this issue in the Mu Us Sandyland, a key area for restoration in northern China. We used satellite data, ground measurements, and computer models to track water changes before and after restoration initiatives. Importantly, we also considered how other human activities, including coal mining and farming, affect water resources. We discovered that previous studies may have overestimated water restoration usage by approximately 251% due to the failure to account for the impacts of other activities. This research helps us better understand how restoring landscapes affects water resources in dry areas, which is crucial for planning sustainable environmental projects worldwide.

## 1. Introduction

Large-scale ecological restoration (ER) of degraded lands has emerged as a critical strategy for enhancing ecosystem services and ensuring environmental security at global scales (Feng et al., 2013). Since 1998, China has initiated an unprecedented series of ER programs, aiming at combating soil erosion, desertification, and climate change while improving dryland ecosystems (Bryan et al., 2018; Lü et al., 2015; Ouyang et al., 2016). Initiatives such as the Three-North Shelterbelt Development Program and the Grain for Green Program have significantly increased vegetation greenness and land improvement (Deng et al., 2014; Mu et al., 2022). However, the success of these programs has led to an unexpected consequence: the intensification of evapotranspiration (ET) due to increased vegetation cover. This has resulted in a decrease of soil water storage and groundwater levels, ultimately reducing the total terrestrial water storage (TWS) and exacerbating water scarcity in affected regions (Deng et al., 2016; Feng et al., 2016; Jia et al., 2017; Lu et al., 2018; Zastrow, 2019; Zhao et al., 2020).

The reduction in TWS poses significant challenges for both socioeconomic development and the protection of water supplies for human and ecosystem needs (Cosgrove & Loucks, 2015). However, some studies suggest that large-scale vegetation recovery may enhance the atmospheric water cycle and increase precipitation through ecosystem feedback mechanisms, potentially mitigating some of the impacts on water resources (Chen et al., 2023; Hoek Van Dijke et al., 2022; Tian et al., 2022; Zhang et al., 2023). Given these complex interactions, accurately quantifying changes in TWS and the impact of ER is crucial for ensuring sustainable water resource management in restoration practices, particularly in water-limited drylands.

To address this challenge, researchers have utilized gravity field measurements from the Gravity Recovery and Climate Experiment (GRACE) satellite, combined with multiple other environmental observations, to estimate changes in TWS and the impact of ER (An et al., 2021; Rodell et al., 2018; Tapley et al., 2019; Zhao et al., 2020). GRACE provides monthly anomalies in the Earth's gravitational field with unprecedented precision (Li et al., 2022; Tapley et al., 2004). While these gravitational variations are primarily driven by water redistribution at monthly scales (Tapley et al., 2004), it is essential to consider other anthropogenic impacts, such as reservoir regulation, water diversion, and bulk commodity transport, when interpreting GRACE data in regions with intensive human activities (Tang et al., 2013; Xie et al., 2018; Zhou et al., 2023). Previous studies have shown that in some regions, such as the North China Plain, the mass-loss rate of groundwater depletion observed by GRACE is significantly offset by mass gains from reservoir regulation, water diversion, and coal transport (Tang et al., 2013). This underscores the necessity of adopting a more comprehensive approach to estimating TWS changes, one that considers region-specific anthropogenic impacts on mass variations.

Our study focused on the Mu Us Sandyland (MUS) and its surrounding areas in northern China (Figures 1a and 1b), a semiarid region that has undergone over 20 years of large-scale ER practices. This area is regarded as one of the most successful examples of vegetation recovery and desertification reversal worldwide (Han et al., 2020; Zhang & Wu, 2020; Zheng et al., 2020). Satellite observations of the Normalized Difference Vegetation Index (NDVI) from 1981 to 2022 revealed a fluctuating yet overall upward trend, rising from 0.15 in 1981 to 0.22 in 2022 (Figures 1c and 1d). Annual land cover data indicated a rapid decrease in bare land area and an increase in grassland area from 1998 to 2002 (Yang & Huang, 2021; Figure 1e), marking the transition between pre-ER (1981–1997) and post-ER (2003–2022) periods.

Previous studies using GRACE time-series data reported that ER in these regions consumed substantial TWS (Cao et al., 2022; Zhao et al., 2020). This finding has raised concerns among the Chinese government and scientists regarding the sustainable water use in ER programs. However, these estimates are questionable for overlooking other human activities, such as coal mining and agricultural water consumption, which may significantly impact mass variations in the region. To address these limitations and provide a more accurate assessment of ER's impact on TWS, we propose a new analytical framework for examining the impact of ER on the TWS in regions with intensive restoration and human activities (Figure 2). Our approach integrates multiple GRACE satellite solutions, field observations, government reports, and ecohydrological modeling to generate a comprehensive picture of TWS changes from 2003 to 2022.

The uniqueness of this study lies in its holistic approach to disentangling the effects of ER from other anthropogenic impacts on TWS. By considering coal mining and agricultural activities, we aim to provide a more nuanced and accurate assessment of ER's impact on water resources. Our findings will have significant implications for the design and implementation of future ER programs, not only in China but also in other regions facing similar challenges in balancing ER with water resource management.

## 2. Methods

Figure 2 illustrates the approach used to disentangle the effects of ER from those of coal mining and farming on TWS during 2003–2022 period, by combining GRACE data with a water balance approach. The detailed steps are explained below. Note that all variables that lead to TWS loss have negative values, such as coal and water mass flow from mining, ET, and runoff.

### 2.1. Estimate of Original GRACE TWS Changes ($\Delta TWS_{ori}$)

A time series of changes in original GRACE TWS ($\Delta TWS_{ori}$) from 2003 to 2022 was estimated by analyzing five GRACE and GRACE Follow-On (GRACE-FO) solutions, including three standard spherical harmonic (SSH) GRACE solutions (CSR, JPL, and GFZ) and two Mascon solutions (CSR and JPL). Comparison between observed water table data (2018–2022) from 97 wells in MUS (Figure 1b) and derived groundwater changes for various GRACE solutions revealed that CSR and JPL Mascon solutions exhibited the highest correlation with

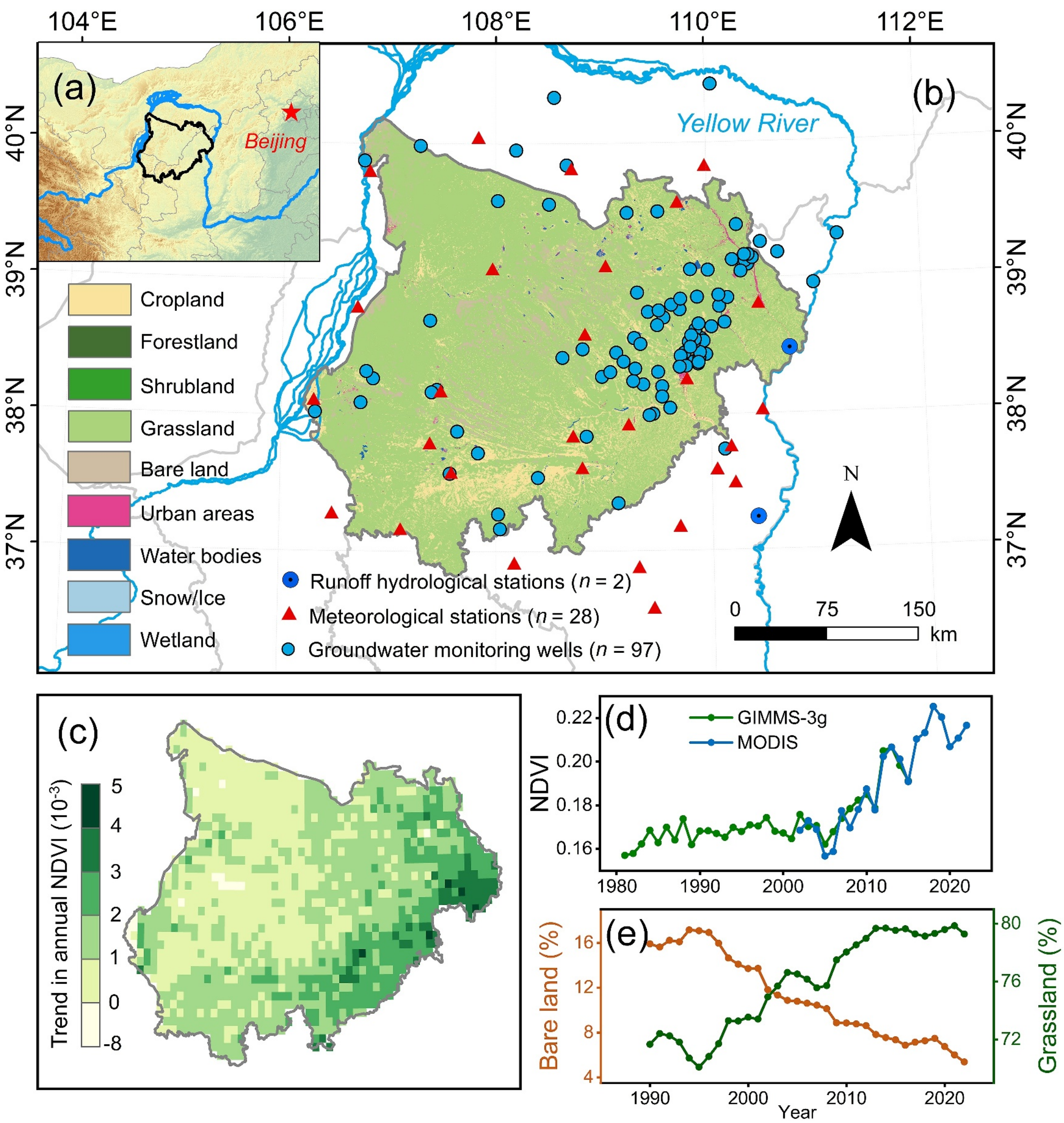


**Figure 1.** Location of MUS and observations. (a) Location of MUS (black polygon); (b) Geographical position of groundwater monitoring wells, meteorological stations, and runoff hydrological stations in the study region; (c) Trend in annual NDVI over MUS during 1981–2022; (d) Annual mean NDVI time series from GIMMS-3g and MODIS averaged over the study region; and (e) Temporal changes in the area percentage of two major land cover types (bare land and grassland) from 1990 to 2022.

measured water table data (Text S1 in Supporting Information S1; Figure S1 in Supporting Information S1). The average of these two solutions was used to calculate the annual changes in TWS of our study area, balancing the strengths of both data sets. Note that GRACE and GRACE-FO have an 11-month data gap (July 2017 to May 2018), which limits the TWS continuity. The Variational Mode Decomposition with Long Short-Term Memory (VMD-LSTM) was used to fill the 11-month data gap between GRACE and GRACE-FO missions (Text S2 in Supporting Information S1; Figures S2 and S3 in Supporting Information S1). Interpolation results closely matched GRACE data, ensuring continuity in our TWS time series (Figure S3 in Supporting Information S1).

### 2.2. Effects of Coal Mining ($TWS_M$) on TWS and Corrected GRACE TWS ($\Delta TWS_{cor}$)

Effects of coal mining on GRACE TWS ($TWS_M$) were calculated by considering both the annual mass loss due to coal mining ($M_{cmf}$) and the associated groundwater co-production ($M_{wmf}$) as:

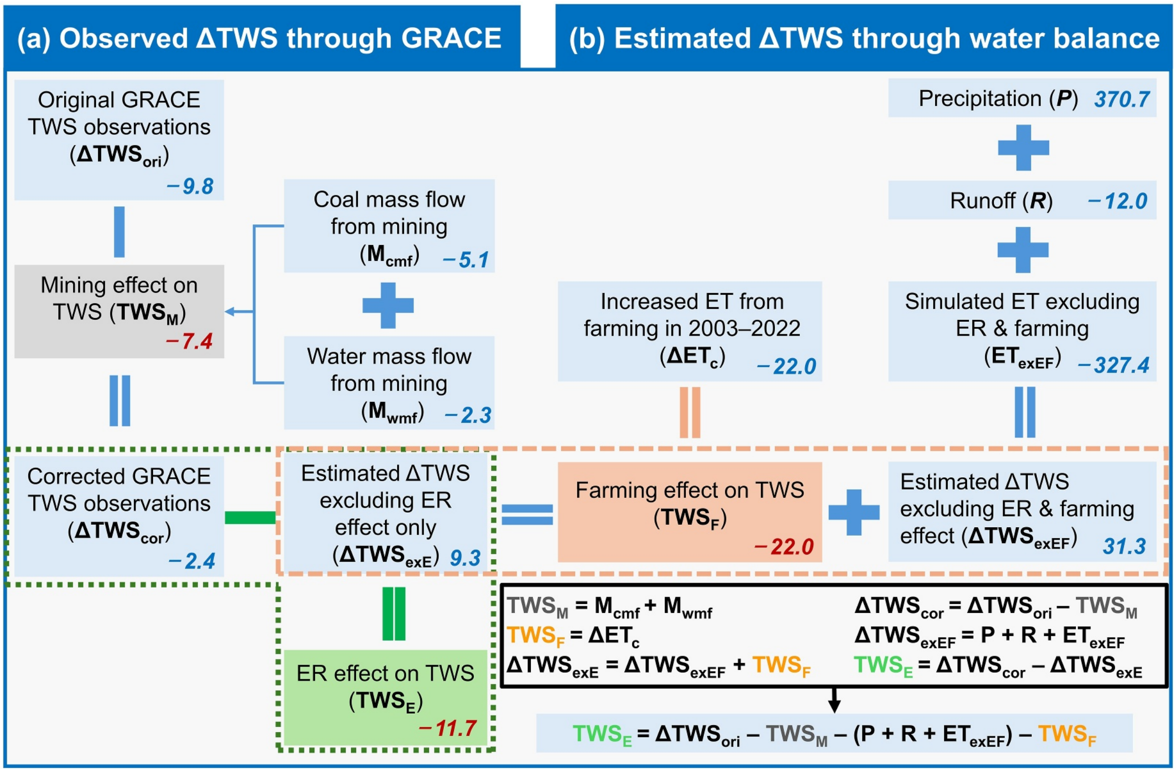


**Figure 2.** Analytical framework to study the potential impact of ER on total TWS. $\Delta TWS_{ori}$ is annual changes in original GRACE TWS. $\Delta TWS_{cor}$ is annual changes in corrected GRACE TWS with coal and water mass flow deductions from mining. $M_{cmf}$ and $M_{wmf}$ are equivalent water thickness of annual coal and water mass flow from mining, respectively. $\Delta TWS_{exEF}$ is the estimated annual changes in TWS with the exclusion of ER and farming. $\Delta TWS_{exE}$ is the estimated TWS trend with the exclusion of ER only. $\Delta ET_c$ is the increased ET from farming. $ET_{exEF}$ is the simulated ET excluding ER and farming impact. $TWS_M$, $TWS_F$ and $TWS_E$ represent impact of mining, farming and ER on TWS, respectively. Bule data represent the multi-year averaged values for each variable and red data represent the effects of various activities on TWS in 2003–2022. Negative values represent the loss of TWS.

$$TWS_M = M_{cmf} + M_{wmf} \tag{1}$$

The annual mass loss due to coal mining (i.e., the amount of raw coal mined) ($M_{cmf}$) (ton yr$^{-1}$) was obtained from China Statistical Yearbook (NBS, 2003–2022) and converted to equivalent water thickness (mm yr$^{-1}$) by assuming water density of 1 ton m$^{-3}$.

During coal mining, significant groundwater volumes are pumped to dewater coal seams (Doulati Ardejani et al., 2011; Mu et al., 2018). This groundwater is discharged directly into surface water runoff or evaporated into the atmosphere. Given the scale of coal production in the study region, both coal transport and the associated water co-production are major sources of mass loss. Groundwater consumption for coal mining can be estimated using the water consumption coefficient per ton of coal (Xie et al., 2018) as:

$$M_{wmf} = \frac{\mu M_{cmf}}{S} \times 1000 \tag{2}$$

where $M_{wmf}$ (mm yr$^{-1}$) is annual groundwater consumption from coal mining, μ (m$^3$ ton$^{-1}$) is water consumption coefficient per ton of coal with an average value of 0.45 m$^3$ ton$^{-1}$ from 25 coal mines in MUS (Zhang et al., 2013), $M_{cmf}$ (ton yr$^{-1}$) is the annual mass loss due to coal mining, $S$ is the area of the study region (m$^2$), and 1000 is the coefficient to convert meters to millimeters.

After removing the effects of mining activities, the corrected annual changes in GRACE TWS ($\Delta TWS_{cor}$) from 2003 to 2022 was calculated as:

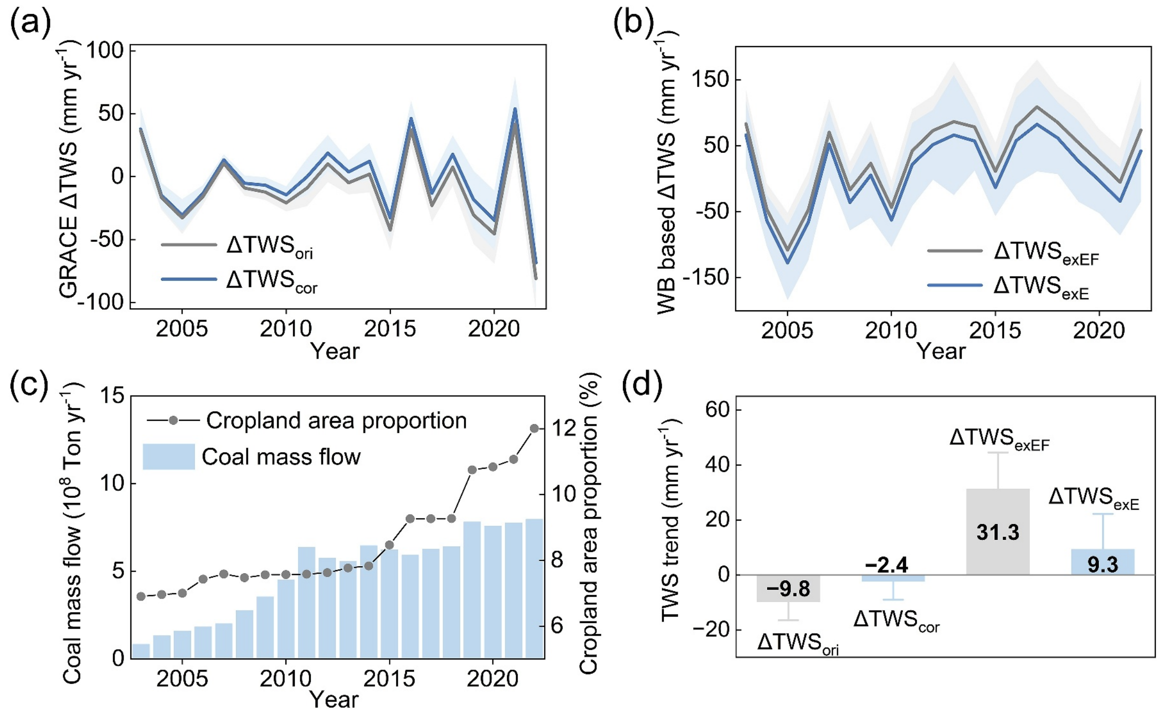


**Figure 3.** Impact of coal mining, farming, and ER on TWS. (a) Annual changes in original TWS ($\Delta TWS_{ori}$) and TWS with coal and water mass flow corrections ($\Delta TWS_{cor}$) using GRACE solutions from 2003 to 2022. The shaded area represents ±1sd; (b) Annual changes in TWS from 2003 to 2022 excluding ER and farming effect ($\Delta TWS_{exEF}$) and TWS excluding ER effect only ($\Delta TWS_{exE}$). The shaded area represents ±1sd; (c) Blue bars represent annual coal mass flow from 2003 to 2022, and gray points represent annual cropland area proportion during the study period; (d) Comparison between observed and simulated multi-year averaged TWS trend during post-ER period 2003–2022.

$$\Delta TWS_{cor} = \Delta TWS_{ori} - TWS_{M} \tag{3}$$

### 2.3. Effects of Farming ($TWS_F$) on the TWS

Cropland area in the study region increased by 5.2% (from 6.9% to 12.1%) over the past 20 years (Figure 3c and Figure S4 in Supporting Information S1). After irrigation with groundwater, excess water is often replenished back into the aquifer, the net effect of agricultural activities on TWS is primarily from ET (Kendy et al., 2004; Zou et al., 2017). Therefore, the effect of farming on the TWS ($TWS_F$) during 2003–2022 period was calculated as:

$$TWS_F = \Delta ET_c \times \frac{S_c}{S} = (ET_c - ET_{exEF}) \times \frac{S_c}{S} \tag{4}$$

where $\Delta ET_c$ (mm yr$^{-1}$) is the increased ET from farming, $ET_c$ (mm yr$^{-1}$) is cropland ET, $ET_{exEF}$ is the simulated ET of natural land without considering ER and farming (see Section 2.4), $S_c$ and $S$ is the area of cropland and the entire study region, respectively.

All croplands in the study region are irrigated. Because cropland remains relatively small and sporadically distributed, we calculated the $ET_c$ using the Penman-Monteith equation (Wang et al., 2013; Text S3).

### 2.4. Calculation of 2003–2022 TWS Excluding ER Impact ($\Delta TWS_{exE}$)

We first calculated the annual changes in TWS during 2003–2022 period excluding ER and farming ($\Delta TWS_{exEF}$). Subsequently, the associated changes in TWS excluding only ER ($\Delta TWS_{exE}$) were determined by incorporating the farming effects (Equation 4) into the TWS values that exclude both ER and farming, as follows:

$$\Delta TWS_{exE} = \Delta TWS_{exEF} + TWS_F \tag{5}$$

The $\Delta TWS_{exEF}$ was calculated using the water-balance equation (Wan et al., 2015; Zeng et al., 2012; Zhao et al., 2020) as:

$$\Delta TWS_{exEF} = P + R + ET_{exEF} \tag{6}$$

where $P$ is annual precipitation, $R$ is annual runoff, and $ET_{exEF}$ is the annual ET simulated with the modified Shuttleworth-Wallace (S-W) model (Li et al., 2023; Shuttleworth & Wallace, 1985). Runoff data were derived from the Baijiachuan and Wenjiachuan hydrological stations (Figure 1b). Meteorological data (1981–2022), including precipitation, temperature, air pressure, relative humidity, and wind speed were obtained from 28 stations across the study region (Figure 1b). For the land use and vegetation-related parameters of the model, annual average values from the pre-ER period (1981–1997) were used to exclude the impacts of ER and farming activities. The model performance was evaluated using the observed ET data from 54 flux towers across China (Figure S5 in Supporting Information S1), and the detailed calculation procedure are referred in Supporting Information (Text S4 in Supporting Information S1).

### 2.5. Effect of ER ($TWS_E$) on the TWS

The impact of ER ($TWS_E$) on TWS was calculated as:

$$TWS_E = \Delta TWS_{cor} - \Delta TWS_{exE} \tag{7}$$

This can be derived by combining Equations 1–6, yielding:

$$TWS_E = \Delta TWS_{ori} - TWS_M - (P + R + ET_{exEF}) - TWS_F \tag{8}$$

Thus, the effects of ER on the TWS during 2003–2022 were disentangled from those of coal mining and farming, based on the GRACE observations and ecohydrological models (Figure 2).

## 3. Results

Original GRACE TWS observations ($\Delta TWS_{ori}$) indicated an average decreasing trend of $-9.8 \pm 6.7$ mm yr$^{-1}$ from 2003 to 2022 (Figures 3a and 3d). The MUS extracts coal with 341.9 million tons per year (Figure 3c). This net coal mass change in the MUS is equivalent to a TWS loss of approximately $-5.1 \pm 0.6$ mm yr$^{-1}$. After deducing the coal mass flow, the adjusted GRACE-derived TWS trend was $-4.7 \pm 7.0$ mm yr$^{-1}$. In addition, the average groundwater loss due to coal seam dewatering was estimated to be approximately $-2.3 \pm 0.3$ mm yr$^{-1}$. Therefore, after accounting for the total coal mining impact ($TWS_M$), the corrected GRACE-derived TWS decreasing trend ($\Delta TWS_{cor}$) was $-2.4 \pm 6.6$ mm yr$^{-1}$ (Figures 3a and 3d).

The modified S-W model, calibrated with data from 54 flux towers across China (Figure S5 in Supporting Information S1), accurately simulated long-term ET trends (NSE = 0.49, RMSE = 1.9 cm, bias = 3.19; Figure S6a in Supporting Information S1). Despite a minor underestimation of ET, the model demonstrated greater precision in dryland ecosystems (Figure S6b in Supporting Information S1), making it suitable for our study area. During the post-ER period (2003–2022), excluding the effects of ER and farming, the estimated TWS ($\Delta TWS_{exEF}$) based on water-balance equation showed an increasing trend at an average rate of $31.3 \pm 13.2$ mm yr$^{-1}$ (Figures 3b and 3d). The estimated multi-year average cropland $ET_c$, calculated using the Penman-Monteith equation, was approximately 553.3 mm yr$^{-1}$, and the net effect of farming on TWS ($TWS_F$) in the study region is approximately $-22.0 \pm 0.9$ mm yr$^{-1}$. Therefore, the TWS, excluding the effects of ER only ($\Delta TWS_{exE}$), showed an increasing trend at an average rate of $9.3 \pm 12.9$ mm yr$^{-1}$ (Figures 3b and 3d).

By comparing $\Delta TWS_{cor}$ and $\Delta TWS_{exE}$, results showed that ER consumed TWS at an average rate of $-11.7 \pm 12.2$ mm yr$^{-1}$ during 2003–2022 (Figure 3d). Importantly, when coal mining and agricultural water consumption are not accounted for, the apparent ER impact on TWS (i.e., $\Delta TWS_{ori}$–$\Delta TWS_{exEF}$) is $-41.1 \pm 13.1$ mm yr$^{-1}$, an overestimation of approximately 251%.

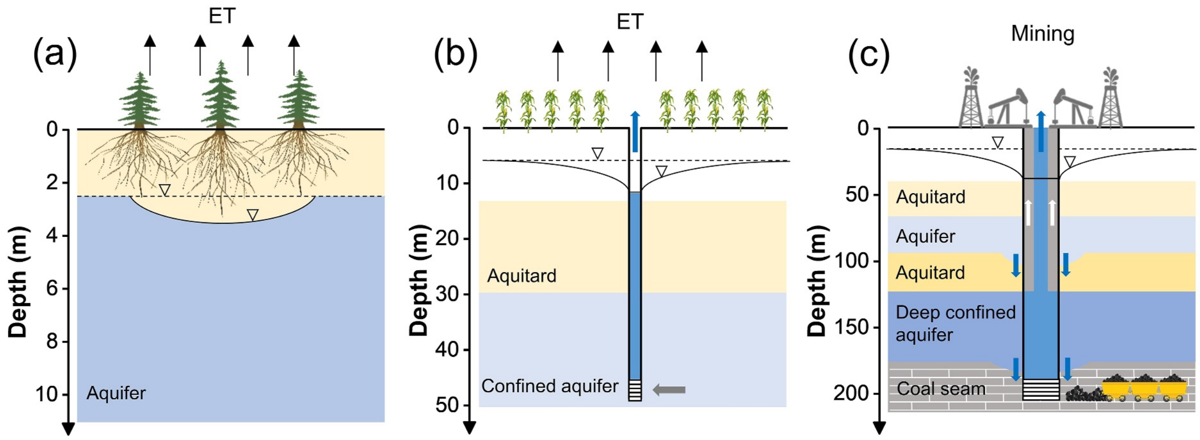


**Figure 4.** Impact factors and mechanisms of TWS in semiarid sandy areas. (a) ER leads to a reduction in water resources through the use of aquifers; (b) Groundwater withdrawal for crop irrigation from aquifers leads to the reduction in water resources. The blue arrow indicates pumping for irrigation; and (c) Mining operations below aquifer cause a drop in the water table because of pumping groundwater for dewatering coal seams. The upward blue arrow represents dewatering coal seams, the downward blue arrows indicate groundwater infiltration due to cracks of the aquifer, and the upward white arrows indicate coal extraction processes. Dashed lines represent the water table before ER, irrigation, and mining, and solid lines represent the water table after various human activities.

## 4. Discussion and Conclusions

Our study presents a novel analytical framework for accurately evaluating the impacts of ER and other human activities on TWS in semiarid regions. By integrating multi-source data and accounting for complex anthropogenic factors, we provide a more nuanced understanding of TWS dynamics and mechanisms in the MUS (Figure 4), with implications for water resource management in similar regions worldwide.

### 4.1. Feasibility of the Analytical Framework

We found that failing to account for the mass-loss from coal mining and transport resulted in a substantial overestimation of water depletion. The importance of this correction is evident when comparing our adjusted GRACE-derived TWS change (mean = $-2.4$ mm yr$^{-1}$) with ground-based shallow aquifer measurements (mean = $-2.7$ mm yr$^{-1}$) in Yellow River Water Resource Bulletins (YRCC, 2003–2022). The close agreement validates our approach and highlights the potential for misinterpretation when relying solely on uncorrected GRACE data. Our findings have broad implications for TWS studies in regions with significant mining or other mass-altering activities, emphasizing the need for a more comprehensive approach to satellite-based water resource assessments.

### 4.2. Reassessing ER Impact on Water Resources

After accounting for coal mining and agricultural activities, we found that ER reduced TWS at a rate of $11.7 \pm 12.2$ mm yr$^{-1}$ during 2003–2022, which is lower than earlier estimates (Zhao et al., 2020). This finding challenges the prevailing narrative of a looming water resource crisis caused by large-scale ER programs. The reduced impact can be attributed to the Chinese government's strategic selection of water-saving tree species and the predominant use of grassland and native shrubs in restoration efforts. For instance, the average multi-year ET of shrubs in MUS (294 mm) is significantly lower than the multi-year average precipitation (402 mm) (Han et al., 2023). This water-conservative approach allows for natural replenishment of water resources consumed by vegetation, minimizing the net impact on regional water availability. Moreover, ER may not result in continued water resource depletion over time. The observed recovery of soil water content with increasing tree age indicates that restored ecosystems and individual plants adapt to water stress conditions, potentially leading to long-term stability in water use (Jia et al., 2017, 2020; Wang et al., 2024).

Note that the potential positive feedback of ER to precipitation was not considered in this study, as the contribution of local ER to enhanced precipitation remains uncertain in the relatively small area. The precipitation trend during post-ER period (2003–2022) in MUS shows an increase of 4.2 mm yr$^{-1}$. Regional and global analyses indicate that ER may have contributed to the increased precipitation in the study area, with estimated increases of

0.85 mm $yr^{-1}$ (Tian et al., 2022) and 1.6 mm $yr^{-1}$ (Hoek Van Dijke et al., 2022), respectively. Consequently, the negative impact of ER on TWS is expected to be further mitigated if the feedback effect is taken into account.

### 4.3. Challenges in Agricultural Water Consumption and Groundwater Management

While our study provides a more optimistic perspective on the impacts of ER, it also highlights critical challenges in agricultural water consumption and groundwater management. First, our results indicate that agricultural water consumption is a primary factor for TWS loss over MUS. This is attributed to the relatively shallow and abundant groundwater resources in the study region, which serves as the primary source for irrigation (Huo et al., 2016; Li et al., 2021b). Second, in recent years, the local government has introduced the "Requisition-Compensation Balance" initiative, a policy that has incentivized local farmers to engage in the reclamation of arable land, leading to a significant expansion of cultivated areas (Gao et al., 2024).

Additionally, the observed rapid decline in the water table (Figure S7 in Supporting Information S1), particularly near agricultural and mining areas, highlights localized issues of overexploitation and disturbance that may not be fully captured by regional-scale TWS assessments. The discrepancy between GRACE-derived TWS trends and site groundwater measurements underscores the complexity of water resource dynamics in heavily modified landscapes. Our findings suggest that water table decline in the region may be more strongly influenced by groundwater withdrawal for agricultural irrigation and mining-induced aquifer disruption than by ER activities. Mining activities conducted below the water table not only requires dewatering but also may disrupt aquifers and cause mining-induced cracks (Zhang et al., 2016), resulting in neighboring observation wells showing an exaggerated drop in water table (Figure 4c). This emphasizes the need for targeted groundwater monitoring and management strategies, particularly in areas with intensive human activity.

### 4.4. Global Implications and Future Directions

Our study demonstrates the importance of a holistic approach to water resource assessment that considers multiple anthropogenic factors. The analytical framework developed here can be applied to other regions with intense human activity, providing a more accurate evaluation of TWS trends globally. This approach is particularly relevant as countries worldwide implement large-scale ER projects to address climate change and land degradation. The findings challenge the notion that ER programs inevitably lead to water resource depletion, offering a more nuanced perspective on the water-vegetation relationship in semiarid ecosystems. This has important implications for global restoration efforts, suggesting that carefully planned and managed ER programs can potentially enhance both ecosystem health and water resource sustainability.

Future research should focus on.

- Refining methods to separate the impacts of various human activities on TWS.
- Investigating long-term adaptation mechanisms of restored ecosystems to water stress.
- Quantifying the feedback effects of large-scale vegetation changes on regional and global water cycles.
- Developing integrated monitoring systems that combine satellite observations with high-resolution ground measurements to provide a more comprehensive understanding of water resource dynamics.

In conclusion, our study provides a more optimistic outlook on the water resource implications of ER in semiarid regions. However, it also highlights the critical need for targeted management of groundwater resources, particularly in areas with intensive agricultural and mining activity. By adopting a more comprehensive approach to water resource assessment and management, we can better handle the complex interactions between human activities, ecosystem restoration, and water availability in a changing climate.

## Conflict of Interest

The authors declare no conflicts of interest relevant to this study.

## Data Availability Statement

Data sets used in this study are collected from various sources: Standard spherical harmonic (SSH) GRACE solutions are available at https://icgem.gfz-potsdam.de/home. GRACE JPL mascon solution is available at https://grace.jpl.nasa.gov/data/get-data/jpl_global_mascons/. GARCE CSR mascon solution is available at https://www2.csr.utexas.edu/grace/RL06_mascons.html. NDVI during 1981–2015 from GIMMS-3g are available at https://climatedataguide.ucar.edu/climate-data/ndvi-normalized-difference-vegetation-index-3rd-generation-nasagfsc-gimms. NDVI during 2002–2022 from MODIS are available at Didan (2015). $CO_2$ concentration data are derived from Lan et al. (2025). LAI during 2002–2022 from MODIS are available at Myneni et al. (2021). LAI during 1981–2010 from AVHRR are available at http://www.glass.umd.edu/Download.html. The storage of plant canopy surface water, soil water, and snow water are available at Beaudoing and Rodell (2020). The ET data from flux tower observations are obtained at FLUXNET (https://fluxnet.org/data/fluxnet2015-dataset/), ChinaFLUX (http://www.nesdc.org.cn/theme/index?projectId=64e80ed07e2817429fbc7b09), and CERN (http://www.cnern.org.cn/data/initDRsearch?classcode=STA). Soil hydraulic parameters data are derived from Zhang et al. (2018).

**Acknowledgments**
This study was supported by the National Natural Science Foundation of China (U2444217 and 42307456), the Strategic Priority Research Program of the Chinese Academy of Sciences (XDB40020000), the GDAS' Project of Science and Technology Development (2021GDASYL-20210102008), and the project "CERN long-term observation data mining and annual data report" (Grant KFJ-SW-YW043).

## References

An, L., Wang, J., Huang, J., Pokhrel, Y., Hugonnet, R., Wada, Y., et al. (2021). Divergent causes of terrestrial water storage decline between drylands and humid regions globally. *Geophysical Research Letters*, *48*(23), e2021GL095035. https://doi.org/10.1029/2021GL095035

Beaudoing, H., & Rodell, M. (2020). GLDAS noah land surface model L4 monthly 0.25 x 0.25 degree V2.1 [Dataset]. *Goddard Earth Sciences Data and Information Services Center (GES DISC)*. https://doi.org/10.5067/SXAVCZFAQLNO

Bryan, B. A., Gao, L., Ye, Y., Sun, X., Connor, J. D., Crossman, N. D., et al. (2018). China's response to a national land-system sustainability emergency. *Nature*, *559*(7713), 193–204. https://doi.org/10.1038/s41586-018-0280-2

Cao, Y., Xie, Z., Woodgate, W., Ma, X., Cleverly, J., Pang, Y., et al. (2022). Ecohydrological decoupling of water storage and vegetation attributed to China's large-scale ecological restoration programs. *Journal of Hydrology*, *615*, 128651. https://doi.org/10.1016/j.jhydrol.2022.128651

Chen, S., Tian, L., Zhang, B., Zhang, G., Zhang, F., Yang, K., et al. (2023). Quantifying the impact of large-scale afforestation on the atmospheric water cycle during rainy season over the Chinese Loess Plateau. *Journal of Hydrology*, *619*, 129326. https://doi.org/10.1016/j.jhydrol.2023.129326

Cosgrove, W. J., & Loucks, D. P. (2015). Water management: Current and future challenges and research directions. *Water Resources Research*, *51*(6), 4823–4839. https://doi.org/10.1002/2014WR016869

Deng, L., Liu, G., & Shangguan, Z. (2014). Land-use conversion and changing soil carbon stocks in China's "Grain-for-Green"Program: A synthesis. *Global Change Biology*, *20*(11), 3544–3556. https://doi.org/10.1111/gcb.12508

Deng, L., Yan, W., Zhang, Y., & Shangguan, Z. (2016). Severe depletion of soil moisture following land-use changes for ecological restoration: Evidence from northern China. *Forest Ecology and Management*, *366*, 1–10. https://doi.org/10.1016/j.foreco.2016.01.026

Didan, K. (2015). MOD13C2 MODIS/Terra vegetation indices monthly L3 global 0.05Deg CMG V006 [Dataset]. *NASA EOSDIS Land Processes Distributed Active Archive Center*. https://doi.org/10.5067/MODIS/MOD13C2.006

Doulati Ardejani, F., Jodieri Shokri, B., Moradzadeh, A., Shafaei, S. Z., & Kakaei, R. (2011). Geochemical characterisation of pyrite oxidation and environmental problems related to release and transport of metals from a coal washing low-grade waste dump, Shahrood, northeast Iran. *Environmental Monitoring and Assessment*, *183*(1–4), 41–55. https://doi.org/10.1007/s10661-011-1904-2

Feng, X., Fu, B., Lu, N., Zeng, Y., & Wu, B. (2013). How ecological restoration alters ecosystem services: An analysis of carbon sequestration in China's Loess Plateau. *Scientific Reports*, *3*(1), 2846. https://doi.org/10.1038/srep02846

Feng, X., Fu, B., Piao, S., Wang, S., Ciais, P., Zeng, Z., et al. (2016). Revegetation in China's Loess Plateau is approaching sustainable water resource limits. *Nature Climate Change*, *6*(11), 1019–1022. https://doi.org/10.1038/nclimate3092

Gao, N., Liang, W., Gou, F., Liu, Y., Fu, B., & Lü, Y. (2024). Assessing the impact of agriculture, coal mining, and ecological restoration on water sustainability in the Mu Us Sandyland. *Science of The Total Environment*, *929*, 172513. https://doi.org/10.1016/j.scitotenv.2024.172513

Han, C., Mu, Y., Zha, T., Qin, S., Liu, P., Tian, Y., & Jia, X. (2023). A dataset of ecosystem fluxes in a shrubland ecosystem of Mau Us Sandy Land in Yanchi, Ningxia, China (2012-2016). *Chinese Journal of Plant Ecology*, *47*(9), 1322–1332. https://doi.org/10.17521/cjpe.2023.0001

Han, X., Jia, G., Yang, G., Wang, N., Liu, F., Chen, H., et al. (2020). Spatiotemporal dynamic evolution and driving factors of desertification in the Mu Us Sandy Land in 30 years. *Scientific Reports*, *10*(1), 21734. https://doi.org/10.1038/s41598-020-78665-9

Hoek Van Dijke, A. J., Herold, M., Mallick, K., Benedict, I., Machwitz, M., Schlerf, M., et al. (2022). Shifts in regional water availability due to global tree restoration. *Nature Geoscience*, *15*(5), 363–368. https://doi.org/10.1038/s41561-022-00935-0

Huo, A., Peng, J., Chen, X., Deng, L., Wang, G., & Cheng, Y. (2016). Groundwater storage and depletion trends in the Loess areas of China. *Environmental Earth Sciences*, *75*(16), 1–11. https://doi.org/10.1007/s12665-016-5951-4

Jia, X., Shao, M., Wei, X., Zhu, Y., Wang, Y., & Hu, W. (2020). Policy development for sustainable soil water use on China's Loess Plateau. *Science Bulletin*, *65*(24), 2053–2056. https://doi.org/10.1016/j.scib.2020.09.006

Jia, X., Shao, M., Zhu, Y., & Luo, Y. (2017). Soil moisture decline due to afforestation across the Loess Plateau, China. *Journal of Hydrology*, *546*, 113–122. https://doi.org/10.1016/j.jhydrol.2017.01.011

Kendy, E., Zhang, Y., Liu, C., Wang, J., & Steenhuis, T. (2004). Groundwater recharge from irrigated cropland in the North China Plain: Case study of Luancheng County, Hebei Province, 1949–2000. *Hydrological Processes*, *18*(12), 2289–2302. https://doi.org/10.1002/hyp.5529

Lan, X., Tans, P., & Thoning, K. W. (2025). Trends in globally-averaged $CO_2$ determined from NOAA global monitoring laboratory measurements (version 2025-01) [Dataset]. *Global Monitoring Laboratory*. https://doi.org/10.15138/9N0H-ZH07

Li, H., Han, S., Wu, X., Wang, S., Liu, W., Ma, T., et al. (2021b). Distribution, characteristics and influencing factors of fresh groundwater resources in the Loess Plateau, China. *China Geology*, *4*(3), 509–526. https://doi.org/10.31035/cg2021057

Li, X., Long, D., Scanlon, B. R., Mann, M. E., Li, X., Tian, F., et al. (2022). Climate change threatens terrestrial water storage over the Tibetan Plateau. *Nature Climate Change*, *12*(9), 801–807. https://doi.org/10.1038/s41558-022-01443-0

Li, Y., Zhang, B., Shao, R., Su, T., Wang, X., Tian, L., & He, C. (2023). Estimating the maximum vegetation coverage and productivity capacity supported by rainwater resources on the Loess Plateau. *Journal of Hydrology*, *619*, 129346. https://doi.org/10.1016/j.jhydrol.2023.129346

Lu, C., Zhao, T., Shi, X., & Cao, S. (2018). Ecological restoration by afforestation may increase groundwater depth and create potentially large ecological and water opportunity costs in arid and semiarid China. *Journal of Cleaner Production*, *176*, 1213–1222. https://doi.org/10.1016/j.jclepro.2016.03.046

Lü, Y., Zhang, L., Feng, X., Zeng, Y., Fu, B., Yao, X., et al. (2015). Recent ecological transitions in China: Greening, browning and influential factors. *Scientific Reports*, *5*(1), 8732. https://doi.org/10.1038/srep08732

Mu, H., Li, X., Ma, H., Du, X., Huang, J., Su, W., et al. (2022). Evaluation of the policy-driven ecological network in the Three-North Shelterbelt region of China. *Landscape and Urban Planning*, *218*, 104305. https://doi.org/10.1016/j.landurbplan.2021.104305

Mu, W., Wu, Q., Xing, Y., Qian, C., Wang, Y., & Du, Y. (2018). Using numerical simulation for the prediction of mine dewatering from a karst water system underlying the coal seam in the Yuxian Basin, Northern China. *Environmental Earth Sciences*, *77*(5), 1–19. https://doi.org/10.1007/s12665-018-7389-3

Myneni, R., Knyazikhin, Y., & Park, T. (2021). MODIS/Terra+Aqua Leaf area Index/FPAR 4-Day L4 global 500m SIN Grid V061 [Dataset]. *NASA EOSDIS Land Processes Distributed Active Archive Center*. https://doi.org/10.5067/MODIS/MCD15A3H.061

NBS (National Bureau of Statistics). (2003–2022). China statistical yearbook. Retrieved from https://www.stats.gov.cn/sj/ndsj/

Ouyang, Z., Zheng, H., Xiao, Y., Polasky, S., Liu, J., Xu, W., et al. (2016). Improvements in ecosystem services from investments in natural capital. *Science*, *352*(6292), 1455–1459. https://doi.org/10.1126/science.aaf2295

Rodell, M., Famiglietti, J. S., Wiese, D. N., Reager, J. T., Beaudoing, H. K., Landerer, F. W., & Lo, M. H. (2018). Emerging trends in global freshwater availability. *Nature*, *557*(7707), 651–659. https://doi.org/10.1038/s41586-018-0123-1

Shuttleworth, W. J., & Wallace, J. (1985). Evaporation from sparse crops-an energy combination theory. *Quarterly Journal of the Royal Meteorological Society*, *111*(469), 839–855. https://doi.org/10.1002/qj.49711146910

Tang, Q., Zhang, X., & Tang, Y. (2013). Anthropogenic impacts on mass change in North China. *Geophysical Research Letters*, *40*(15), 3924–3928. https://doi.org/10.1002/grl.50790

Tapley, B. D., Bettadpur, S., Ries, J. C., Thompson, P. F., & Watkins, M. M. (2004). GRACE measurements of mass variability in the earth system. *Science*, *305*(5683), 503–505. https://doi.org/10.1126/science.1099192

Tapley, B. D., Watkins, M. M., Flechtner, F., Reigber, C., Bettadpur, S., Rodell, M., et al. (2019). Contributions of GRACE to understanding climate change. *Nature Climate Change*, *9*(5), 358–369. https://doi.org/10.1038/s41558-019-0456-2

Tian, L., Zhang, B., Chen, S., Wang, X., Ma, X., & Pan, B. (2022). Large-scale afforestation enhances precipitation by intensifying the atmospheric water cycle over the Chinese Loess Plateau. *Journal of Geophysical Research: Atmospheres*, *127*(16), e2022JD036738. https://doi.org/10.1029/2022JD036738

Wan, Z., Zhang, K., Xue, X., Hong, Z., Hong, Y., & Gourley, J. J. (2015). Water balance-based actual evapotranspiration reconstruction from ground and satellite observations over the conterminous United States. *Water Resources Research*, *51*(8), 6485–6499. https://doi.org/10.1002/2015WR017311

Wang, H., Ma, M., Yu, W., & Huang, G. (2013). Estimation of evapotransipiration of grassland and cropland ecosystems in arid region based on MODIS satellite data and Penman-Monteith equation. In *2013 IEEE international geoscience and remote sensing symposium - IGARSS* (pp. 1763–1766). IEEE. https://doi.org/10.1109/IGARSS.2013.6723139

Wang, Y. Q., Hu, W., Sun, H., Zhao, Y. L., Zhang, P. P., Li, Z., et al. (2024). Soil moisture decline in China's monsoon loess critical zone: More a result of land-use conversion than climate change. *PNAS*, *121*(15), e2322127121. https://doi.org/10.1073/pnas.2322127121

Xie, X., Xu, C., Wen, Y., & Li, W. (2018). Monitoring groundwater storage changes in the Loess Plateau using GRACE satellite gravity data, hydrological models and coal mining data. *Remote Sensing*, *10*(4), 605. https://doi.org/10.3390/rs10040605

Yang, J., & Huang, X. (2021). 30 m annual land cover and its dynamics in China from 1990 to 2019. *Earth System Science Data Discussions*, *13*(8), 3907–3925. https://doi.org/10.5194/essd-13-3907-2021

YRCC (Yellow River Conservancy Commission of the Ministry of Water Resources). (2003–2022). Yellow River Water Resources Bulletin. Retrieved from http://yrcc.gov.cn/gzfw/szygb/index.html

Zastrow, M. (2019). China's tree-planting could falter in a warming world. *Nature*, *573*(7775), 474–475. https://doi.org/10.1038/d41586-019-02789-w

Zeng, Z., Piao, S., Lin, X., Yin, G., Peng, S., Ciais, P., & Myneni, R. B. (2012). Global evapotranspiration over the past three decades: Estimation based on the water balance equation combined with empirical models. *Environmental Research Letters*, *7*(1), 014026. https://doi.org/10.1088/1748-9326/7/1/014026

Zhang, B., Liu, J., Zhang, B., & Ma, Y. (2013). Analysis of the current situation of drainage water discharge in coal mines in Yulin City. *Soil and Water Conservation in China*, *2013*(01), 34–36. https://doi.org/10.14123/j.cnki.swcc.2013.01.003

Zhang, C., Long, D., Liu, T., Slater, L. J., Wang, G., Zuo, D., et al. (2023). Grassland greening and water resource availability may coexist in a warming climate in Northern China and the Tibetan Plateau. *Earth's Future*, *11*(12), e2023EF004037. https://doi.org/10.1029/2023EF004037

Zhang, M., & Wu, X. (2020). The rebound effects of recent vegetation restoration projects in Mu Us Sandy land of China. *Ecological Indicators*, *113*, 106228. https://doi.org/10.1016/j.ecolind.2020.106228

Zhang, Y., Schaap, M. G., & Zha, Y. (2018). A high-resolution global map of soil hydraulic properties produced by a hierarchical parameterization of a physically based water retention model. *Water Resources Research*, *54*(12), 9774–9790. https://doi.org/10.1029/2018WR023539

Zhang, Z., Zhang, Y., Fu, X., Wang, K., Shi, Y., & Shen, X. (2016). Research on the influence of coal mining on aquifer and its prevention technology in Shanxi Province. In *In sustainable development: Proceedings of the 2015 international conference on sustainable development (ICSD2015)* (pp. 931–939). World Scientific. https://doi.org/10.1142/9789814749916_0098

Zhao, M., A, G., Zhang, J., Velicogna, I., Liang, C., & Li, Z. (2020). Ecological restoration impact on total terrestrial water storage. *Nature Sustainability*, *4*(1), 56–62. https://doi.org/10.1038/s41893-020-00600-7

Zheng, Y., Dong, L., Xia, Q., Liang, C., Wang, L., & Shao, Y. (2020). Effects of revegetation on climate in the Mu Us Sandy Land of China. *Science of The Total Environment*, *739*, 139958. https://doi.org/10.1016/j.scitotenv.2020.139958

Zhou, Y., Dong, J., Cui, Y., Zhao, M., Wang, X., Tang, Q., et al. (2023). Ecological restoration exacerbates the agriculture-induced water crisis in North China Region. *Agricultural and Forest Meteorology*, *331*, 109341. https://doi.org/10.1016/j.agrformet.2023.109341

Zou, M., Niu, J., Kang, S., Li, X., & Lu, H. (2017). The contribution of human agricultural activities to increasing evapotranspiration is significantly greater than climate change effect over Heihe agricultural region. *Scientific Reports*, *7*(1), 8805. https://doi.org/10.1038/s41598-017-08952-5

## References From the Supporting Information

Chu, J., Su, X., Jiang, T., Qi, J., Zhang, G., & Wu, H. (2023). Filling the gap between GRACE and GRACE-FO data using a model integrating variational mode decomposition and long short-term memory: A case study of northwest China. *Environmental Earth Sciences*, *82*(1), 38. https://doi.org/10.1007/s12665-022-10716-y

10.1029/2024GL111669

Gyawali, B., Ahmed, M., Murgulet, D., & Wiese, D. N. (2022). Filling temporal gaps within and between GRACE and GRACE-FO terrestrial water storage records: An innovative approach. *Remote Sensing*, *14*(7), 1565. https://doi.org/10.3390/rs14071565

Han, L., Zhang, R., Wang, X., Bao, A., & Jing, H. (2019). Multi-step wind power forecast based on VMD-LSTM. *IET Renewable Power Generation*, *13*(10), 1690–1700. https://doi.org/10.1049/iet-rpg.2018.5781

Lai, Y., Zhang, B., Yao, Y., Liu, L., Yan, X., He, Y., & Ou, S. (2022). Reconstructing the data gap between GRACE and GRACE follow-on at the basin scale using artificial neural network. *Science of the Total Environment*, *823*, 153770. https://doi.org/10.1016/j.scitotenv.2022.153770

Li, F., Kusche, J., Chao, N., Wang, Z., & Löcher, A. (2021a). Long-term (1979-present) total water storage anomalies over the global land derived by reconstructing GRACE data. *Geophysical Research Letters*, *48*(8), e2021GL093492. https://doi.org/10.1029/2021GL093492

Lu, G., & Wong, D. (2008). An adaptive inverse-distance weighting spatial interpolation technique. *Computers & Geosciences*, *34*(9), 1044–1055. https://doi.org/10.1016/j.cageo.2007.07.010

Thornton, P. E., Law, B. E., Gholz, H. L., Clark, K. L., Falge, E., Ellsworth, D. S., et al. (2002). Modeling and measuring the effects of disturbance history and climate on carbon and water budgets in evergreen needleleaf forests. *Agricultural and Forest Meteorology*, *113*(1–4), 185–222. https://doi.org/10.1016/S0168-1923(02)00108-9

Zhong, Y., Feng, W., Zhong, M., & Ming, Z. (2020). *Dataset of reconstructed terrestrial water storage in China based on precipitation (2002–2019)*. National Tibetan Plateau Data Center.